Supporting information

Shape dependent electrocatalytic activity of iridium oxide decorated erbium pyrosilicate towards hydrogen evolution reaction over the entire pH range

Paramita Karfa,[a,*] Kartick C. Majhi,[a] Rashmi Madhuri,[a]

[a]Department of Applied Chemistry, Indian Institute of Technology (Indian School of Mines), Dhanbad, Jharkhand 826 004, INDIA

*Corresponding author: paramitakarfa@gmail.com (P. Karfa), Tel: +91 8250897637.

S1. Instrumentation details

The FE-SEM images, elemental mapping images and elemental table shown in this work were recorded using Field-emission scanning electron microscope (FE-SEM, Zeiss model Supra 55)having elemental imaging and EDAX facility. Ms. Karfa wishes to thank the central research facility of IIT (ISM), Dhanbad for this research facility.All the XRD data reported in this work has been performed on Xpert Pro MPD diffractometer using Cu radiation source (λ = 30mA). Ms. Karfa wishes to thank the Condensed Matter Physics Laboratory, Tata Institute of Fundamental Research (TIFR), India for providing her this research facility.

JEM-1400 Transmission Electron Microscope (TEM) was used for TEM and SAED analysis, while ESCA+ (Omicron Nanotechnology, Oxford Instrument Germany) was the instrument of X-Ray Photoelectron spectroscopy (XPS) equipped with Aluminum Source (Al k radiation hv = 1486.7ev) used for XPS study. Ms. Karfa wishes to acknowledge Spring testing solutions for providing the XPS and TEM facilities.BET analysis was done by micromeritics 3Flex Surface Characterization Analyzer, which is present in central research facility of IIT (ISM), Dhanbad.ICP-MS data was recorded in Agilent ICP-MS 7900, present in the central research facility of IITDelhi. All the Electrochemical measurements were performed on a CH instrument (USA, model number 660C) present in the Department of Applied Chemistry, IIT (ISM), Dhanbad.

Table S1: Synthetic Conditions for preparation of various shaped $Er_2Si_2O_7$:IrO_2.

S. N.	Compound	Shape	TEOS (ml)	CTAB (mg)	Rotation speed (rpm)
1.	$Er_2Si_2O_7$:$IrO_{2\text{-}1}$	Sheet	6.2	10	550
2.	$Er_2Si_2O_7$:$IrO_{2\text{-}2}$	Small sphere	6.2	20	400
3.	$Er_2Si_2O_7$:$IrO_{2\text{-}3}$	Large Sphere	6.2	30	330
4.	$Er_2Si_2O_7$:$IrO_{2\text{-}4}$	Rod	6.2	40	250
5.	$Er_2Si_2O_7$:$IrO_{2\text{-}5}$	Cube	6.2	50	200
6.	$Er_2Si_2O_7$:$IrO_{2\text{-}6}$	No shape	6.2	60	150
7.	$Er_2Si_2O_7$:$IrO_{2\text{-}7}$	Bulk material	6.2	0	600

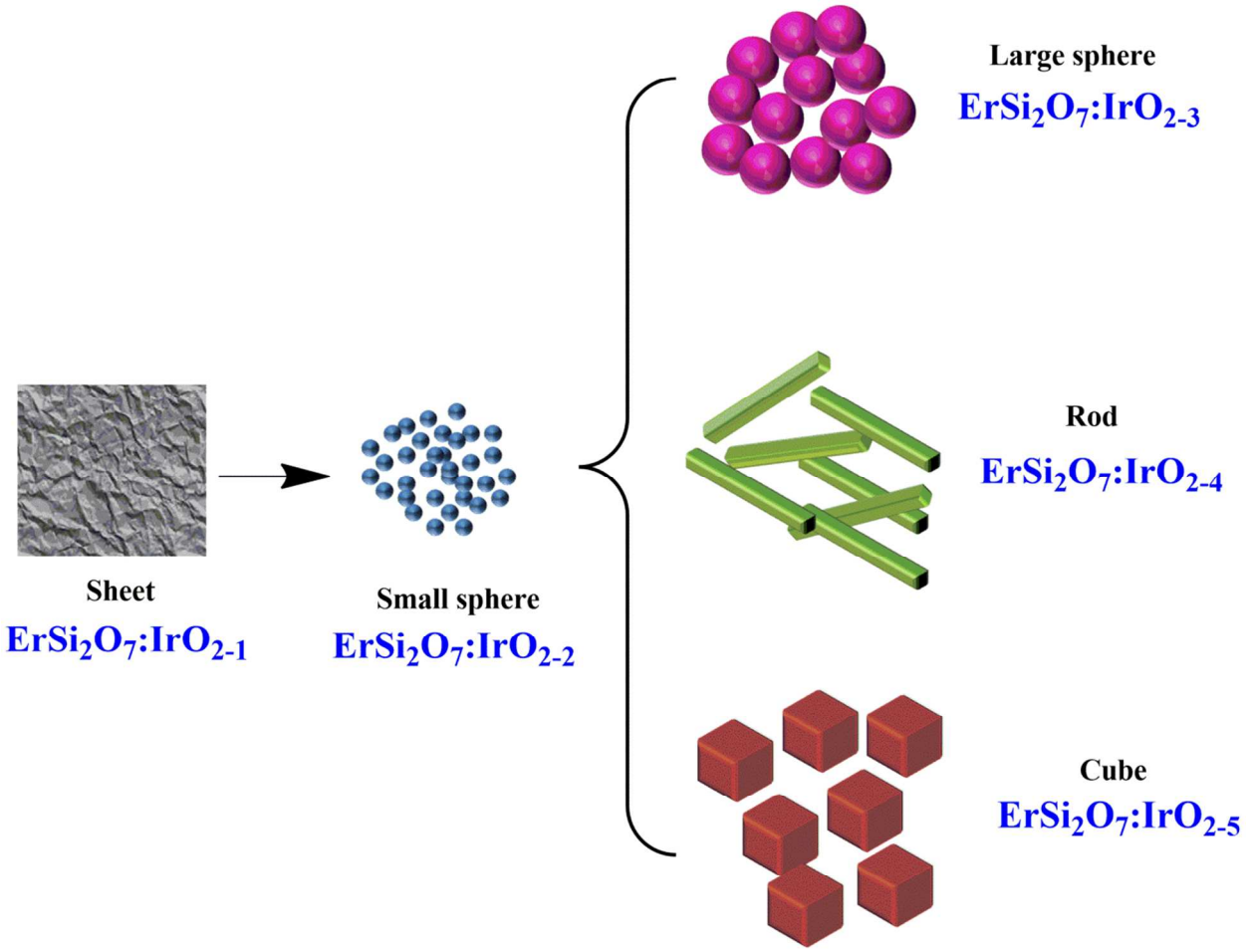

Scheme S1: Graphical representation showing synthesis of different shaped nanocomposites starting from sheet to cube-like structure.

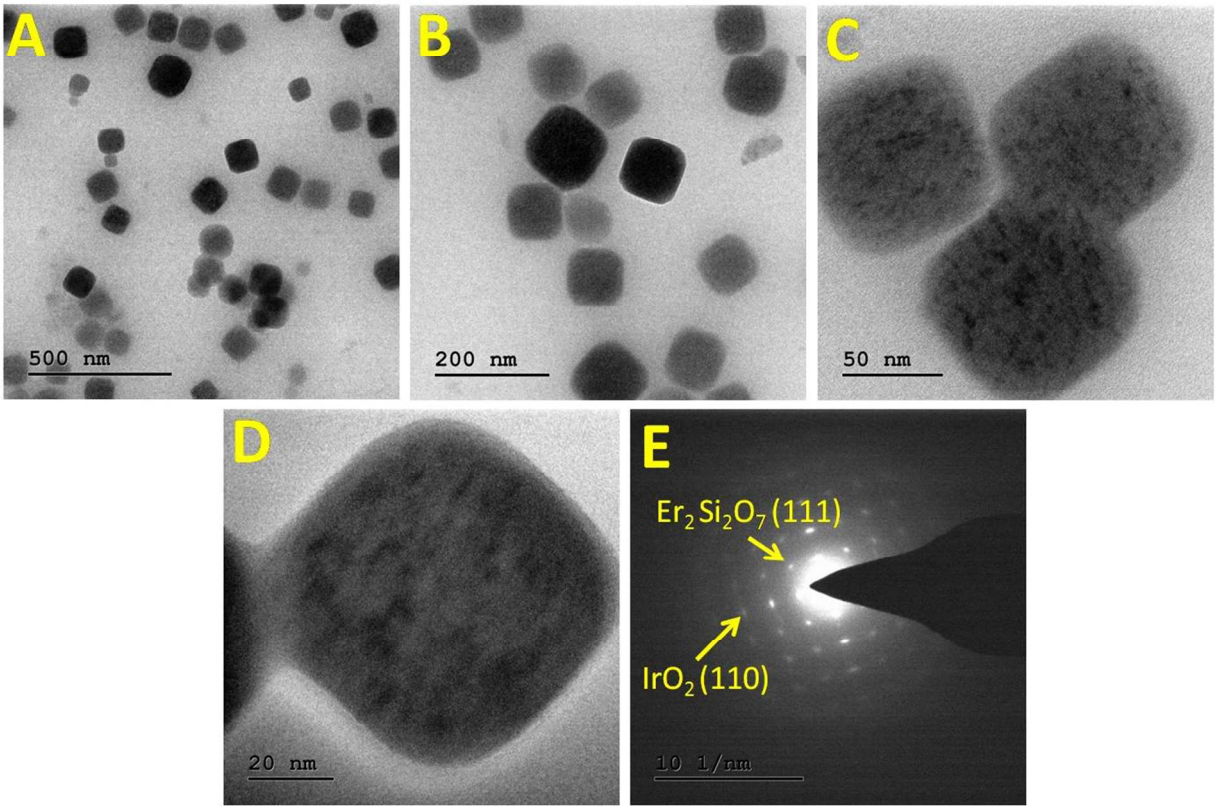

Figure S1: (A to D) TEM images and (E) selected area electron diffraction (SAED) pattern of cube shaped $Er_2Si_2O_7$:$IrO_{2\text{-}5}$.

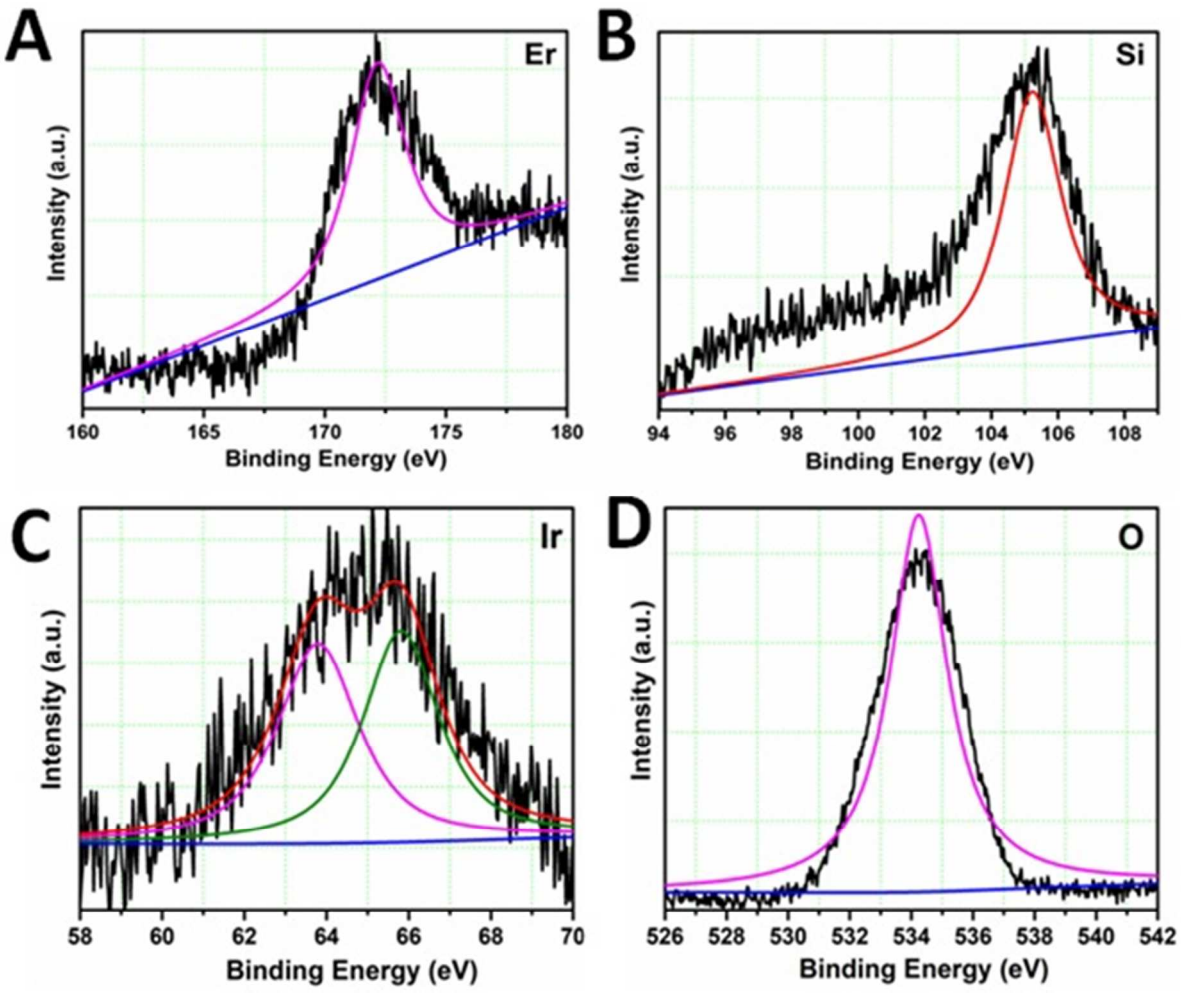

Figure S2: XPS spectra of cube shaped $Er_2Si_2O_7$:IrO_{2-5} for: (A) Er, (B) Si, (C) Ir and (D) O elements.

A

Element	Weight %	Atomic %
O K	33.51	72.88
Si K	12.95	16.05
Er M	51.01	10.61
Ir M	2.52	0.46
Totals	100.00	

B

Element	Weight %	Atomic %
O K	37.94	73.87
Si K	15.85	17.58
Er M	43.98	8.19
Ir M	2.22	0.36
Totals	100.00	

C

Element	Weight %	Atomic %
O K	38.08	74.01
Si K	15.78	17.48
Er M	43.42	8.07
Ir M	2.72	0.44
Totals	100.00	

D

Element	Weight %	Atomic %
O K	37.73	73.54
Si K	16.12	17.90
Er M	44.34	8.27
Ir M	1.81	0.29
Totals	100.00	

E

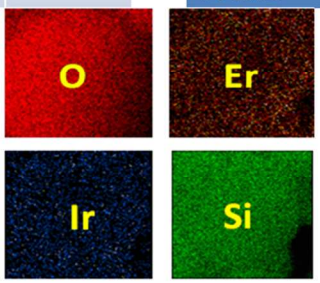

Figure S3: Elemental table of: (A) $Er_2Si_2O_7$:$IrO_{2\text{-}1}$, (B) $Er_2Si_2O_7$:$IrO_{2\text{-}2}$, (C) $Er_2Si_2O_7$:$IrO_{2\text{-}3}$, (D) $Er_2Si_2O_7$:$IrO_{2\text{-}4}$and (E) Elemental mapping for $Er_2Si_2O_7$:$IrO_{2\text{-}5}$.

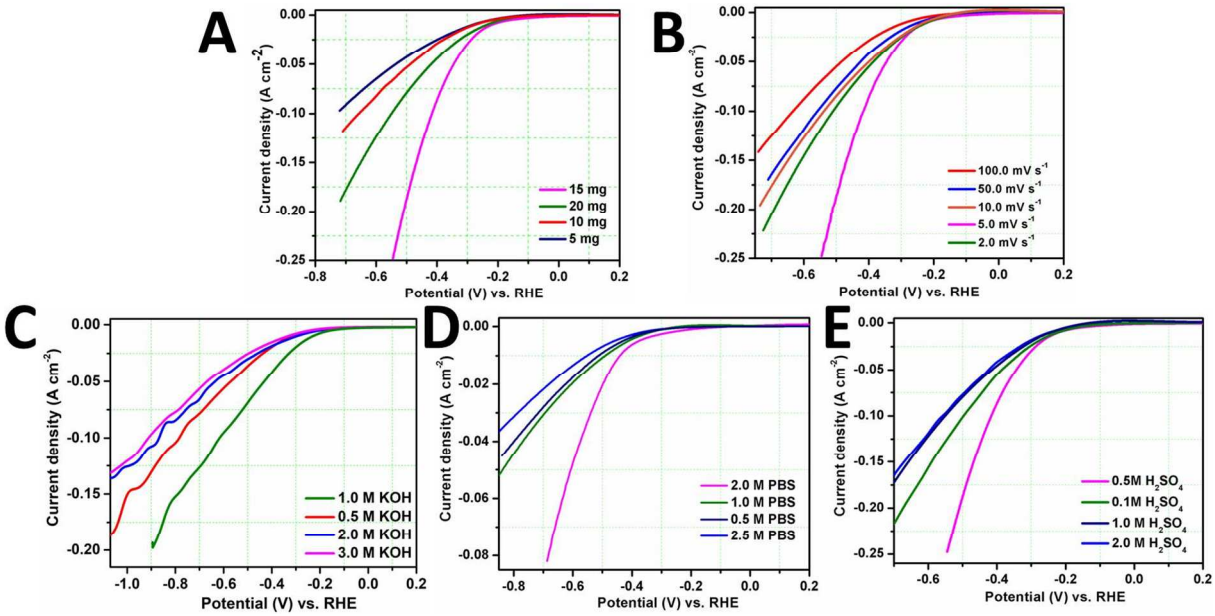

Figure S4: HER LSV run for the optimization of (A) Loading amount, (B) Scan rate, and concentration of Supporting electrolytes i.e. (C) KOH, (D) PBS, and (E) H_2SO_4.

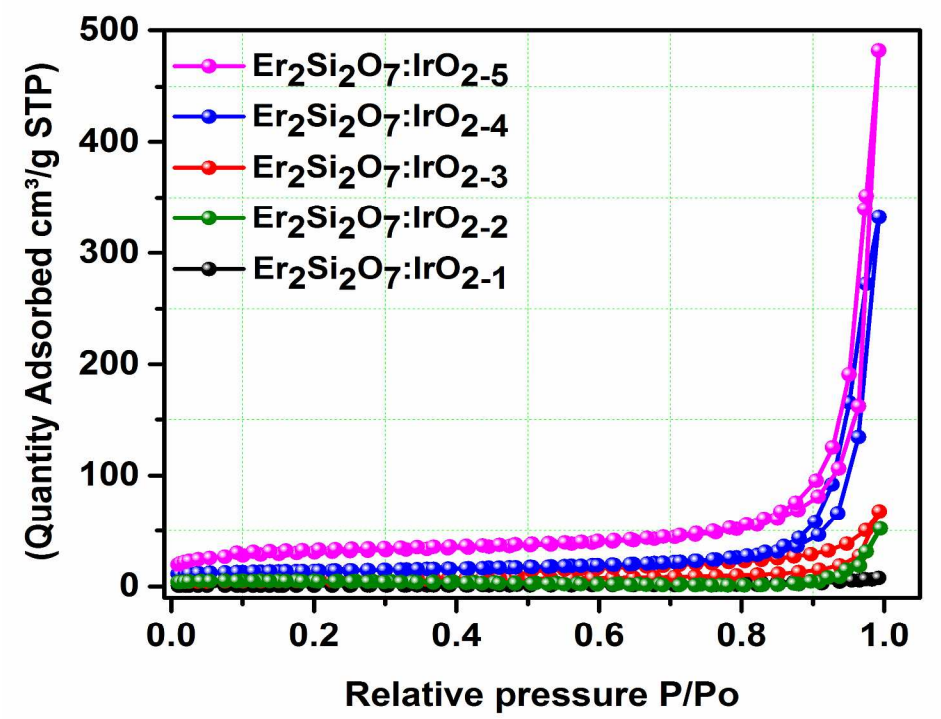

Figure S5: BET N_2 adsorption desorption isotherm of all the nanocomposites.

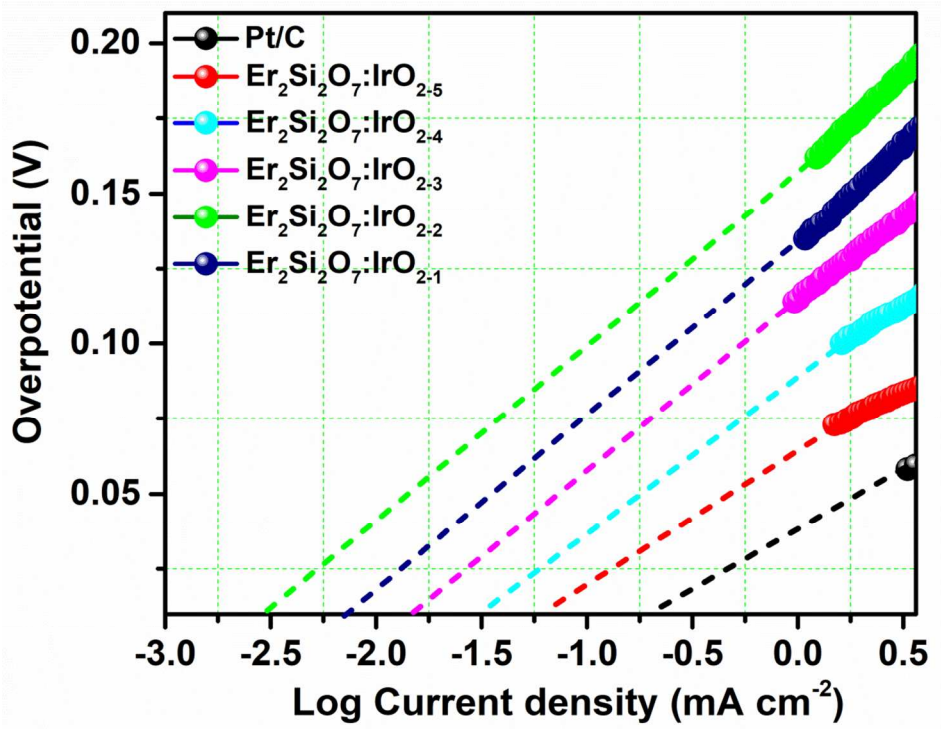

Figure S6: Exchange current density graph of all the nanocomposites by extrapolation of TAFEL plot in acidic medium.

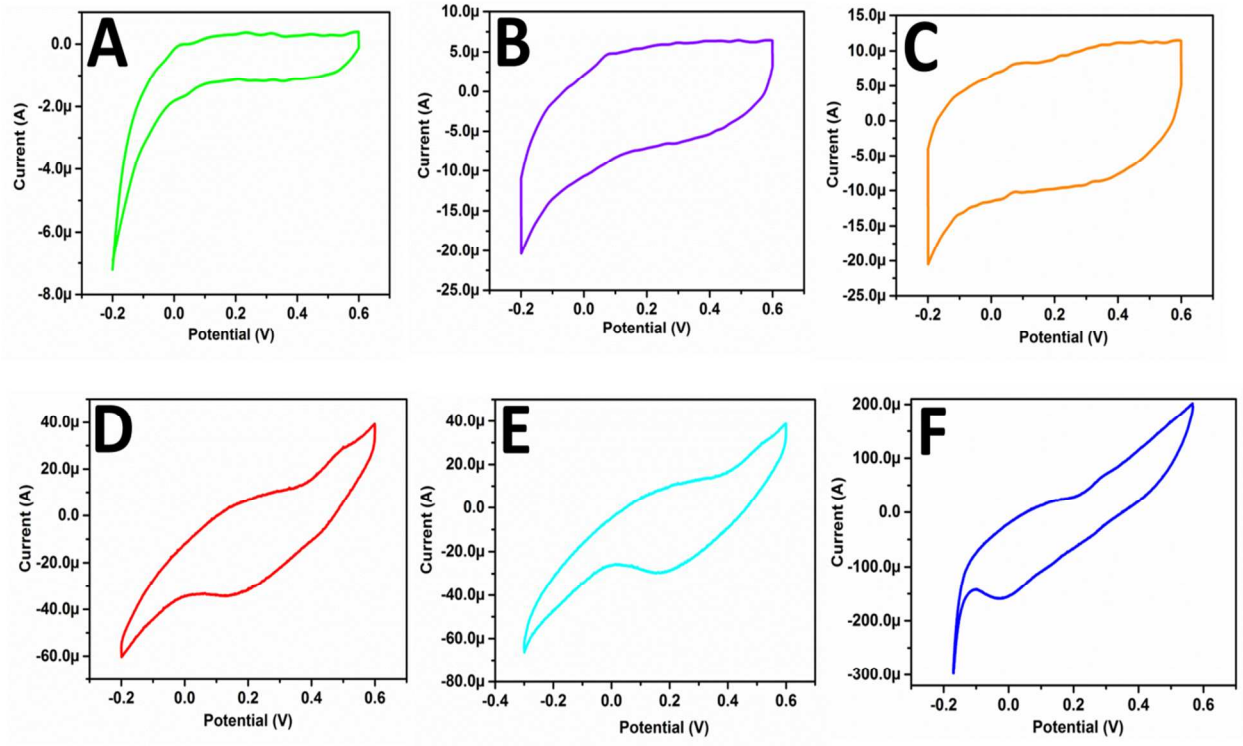

Figure S7: CV of (A) $Er_2Si_2O_7$:$IrO_{2\text{-}4}$, (B) Pt/C, (C) $Er_2Si_2O_7$:$IrO_{2\text{-}3}$, (D) $Er_2Si_2O_7$:$IrO_{2\text{-}2}$, (E) $Er_2Si_2O_7$:$IrO_{2\text{-}1}$, and (F) $Er_2Si_2O_7$:$IrO_{2\text{-}5}$ in 0.5M H_2SO_4 for the calculation of TOF value.

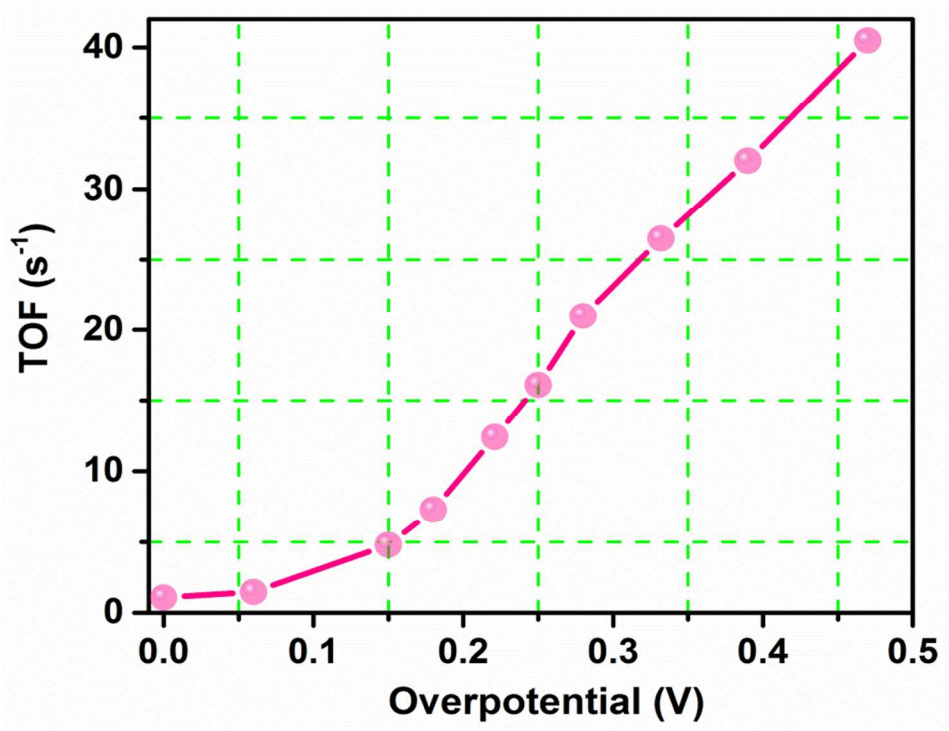

Figure S8: Turn over frequency (TOF) of $Er_2Si_2O_7$:$IrO_{2\text{-}5}$ catalyst with respect to change in overpotential value.

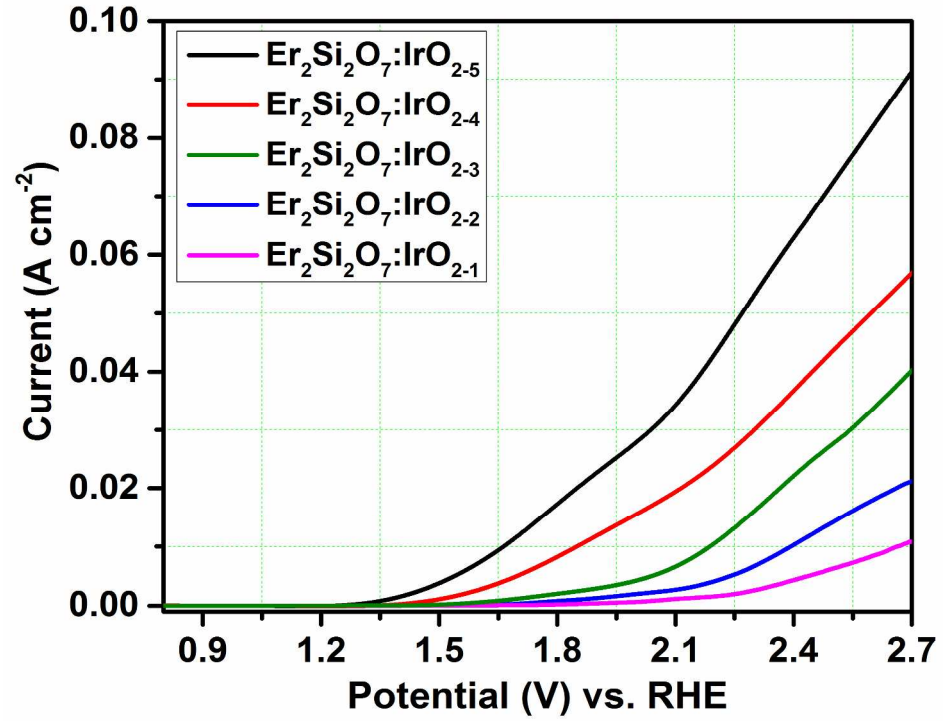

Figure S9: Role of proposed catalysts towards oxygen evolution reaction (OER).

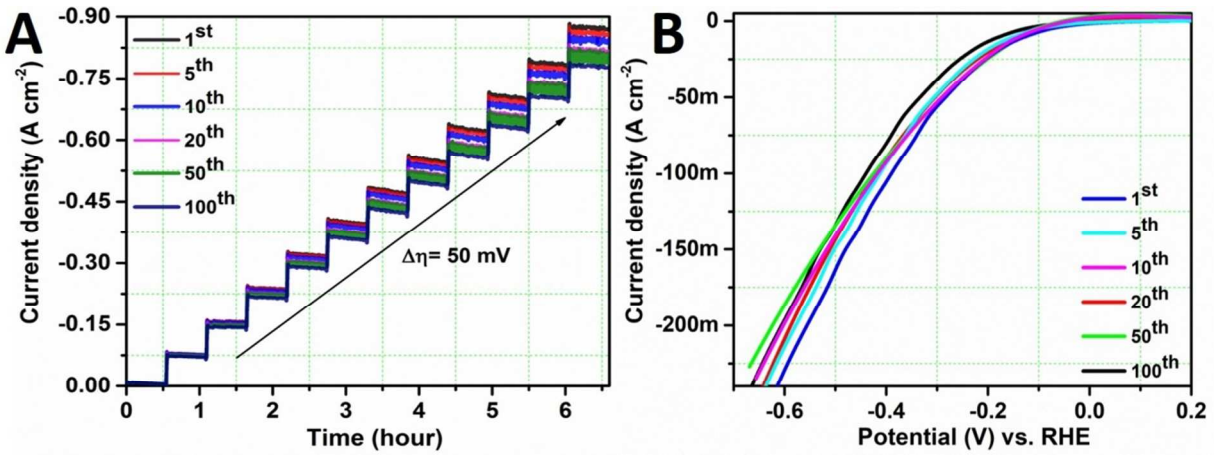

Figure S10:(A) Multi-step chronoamperometric runs for various cycles and (B) corresponding LSV plot for $Er_2Si_2O_7$:$IrO_{2\text{-}5}$ catalyst in acidic medium.

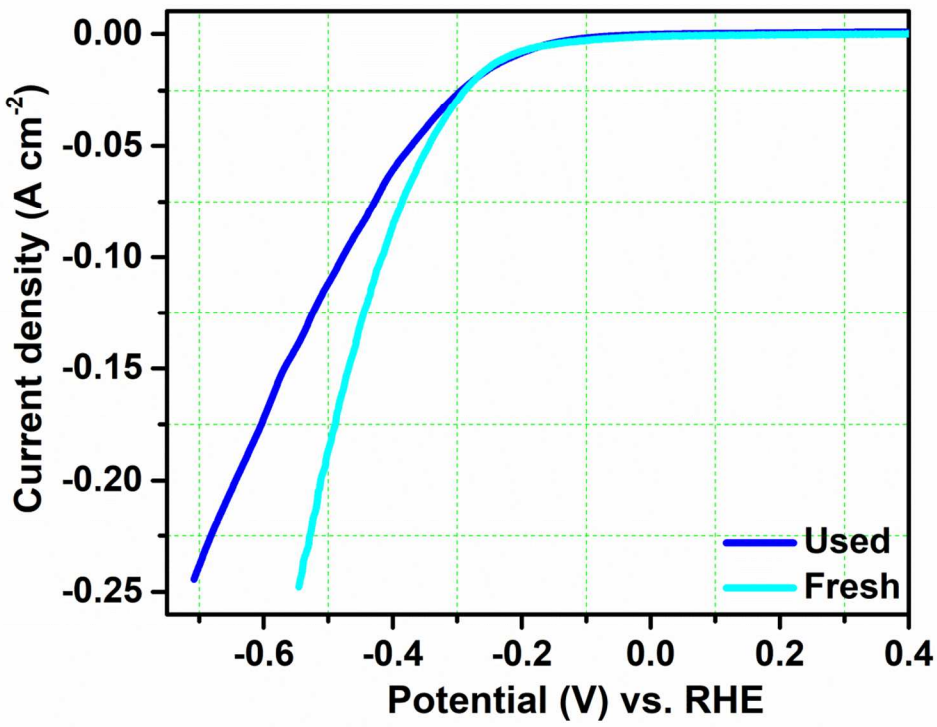

Figure S11: Assessment of electrocatalytic activity between the fresh and used $Er_2Si_2O_7$:$IrO_{2\text{-}5}$ catalyst towards HER in acidic medium.

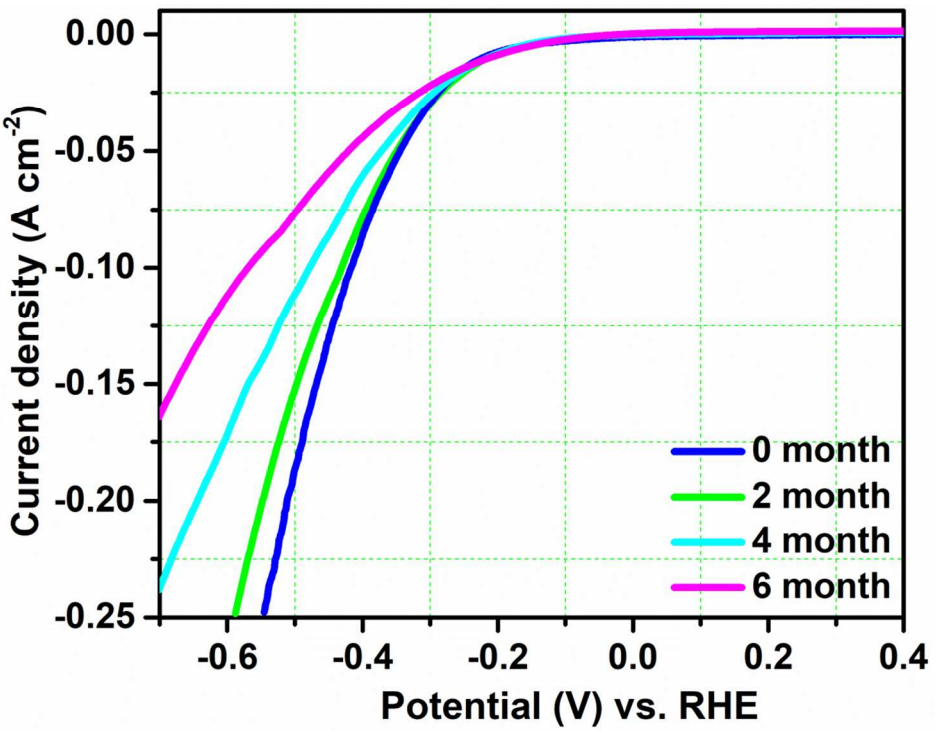

Figure S12: Storage stability of the $Er_2Si_2O_7$:$IrO_{2\text{-}5}$ catalyst toward HER for several months.

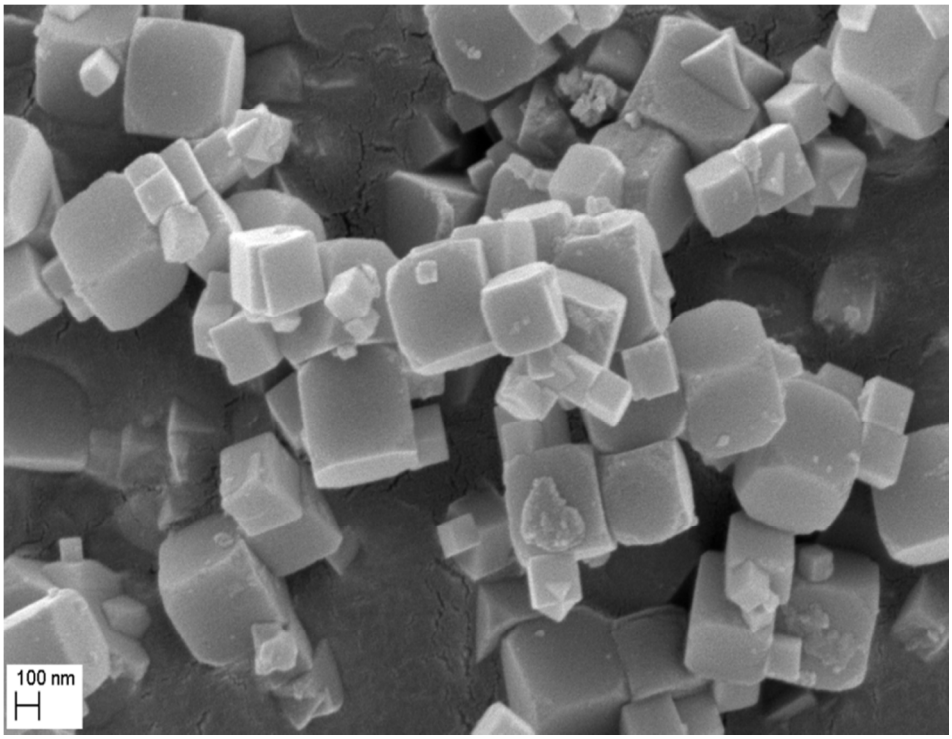

Figure S13: FE-SEM image of the $Er_2Si_2O_7$:$IrO_{2\text{-}5}$ catalyst after several electrochemical studies.

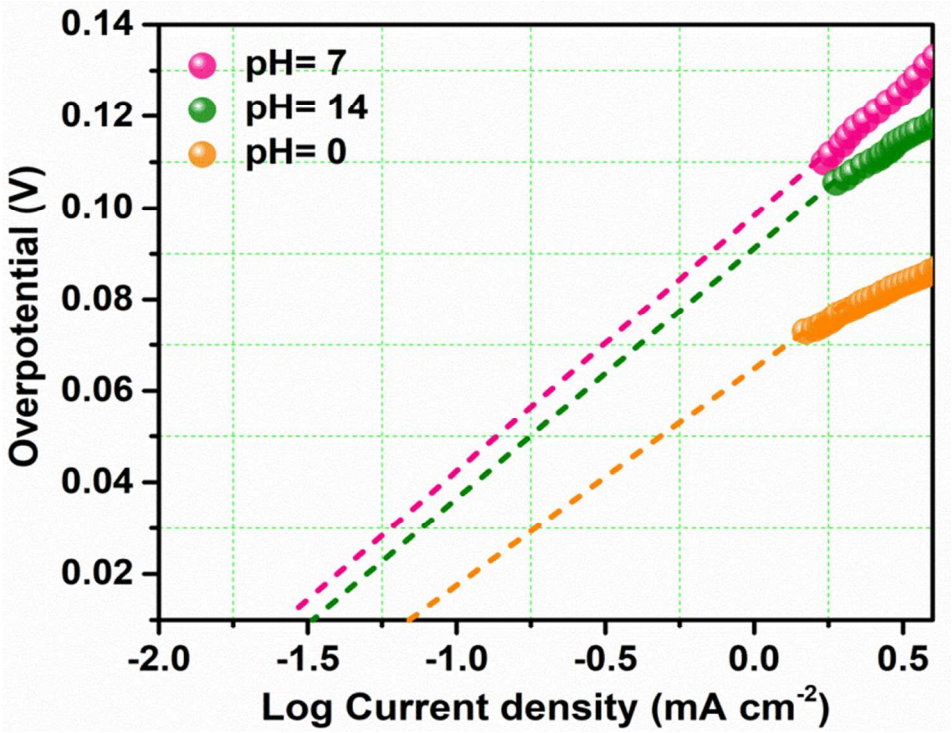

Figure S14: Exchange current density graph of $Er_2Si_2O_7$:IrO_{2-5} by extrapolating TAFEL plot in pH=0, pH=14 and pH=7.

Table S2: Performance of cube-shaped nanocomposite over entire pH range.

S.N.	pH value	Onset potential (V)(η_0)	$\Delta\eta$ (mV)	Tafel slope (mV/dec)	j_o (mA cm^{-2})
1.	pH=0	-0.076	130	49	0.06
2.	pH= 14	-0.090	170	59	0.034
3.	pH= 7	-0.210	190	67	0.026

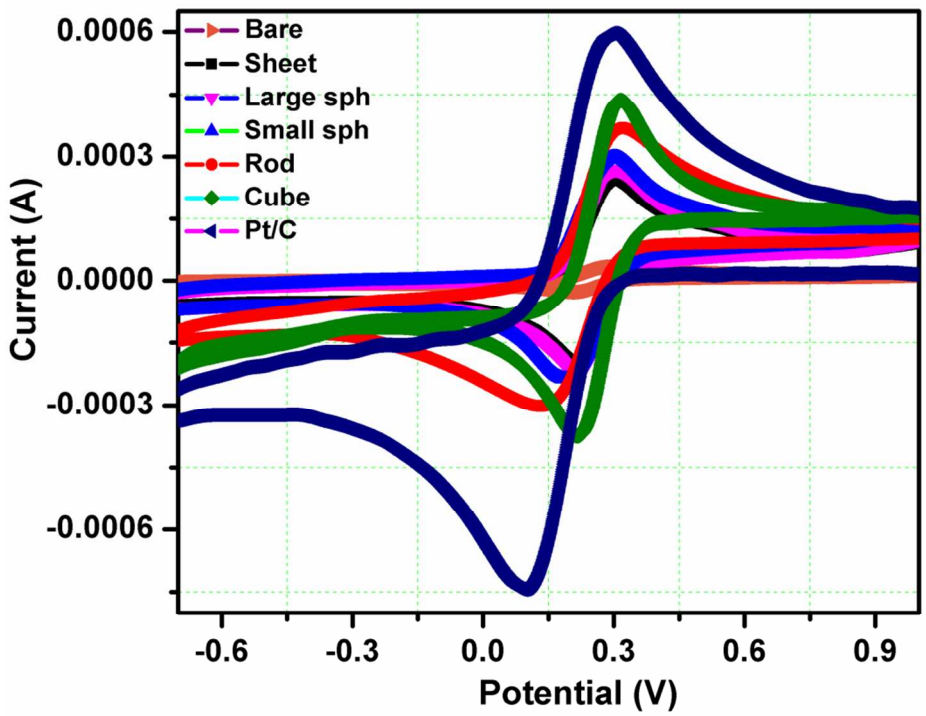

Figure S15:Electrocatalytic activity study using potassium ferrocyanide as an electroactive electrolyte for all the nanocomposites ($Er_2Si_2O_7$:IrO_2), Pt/C and bare electrode.

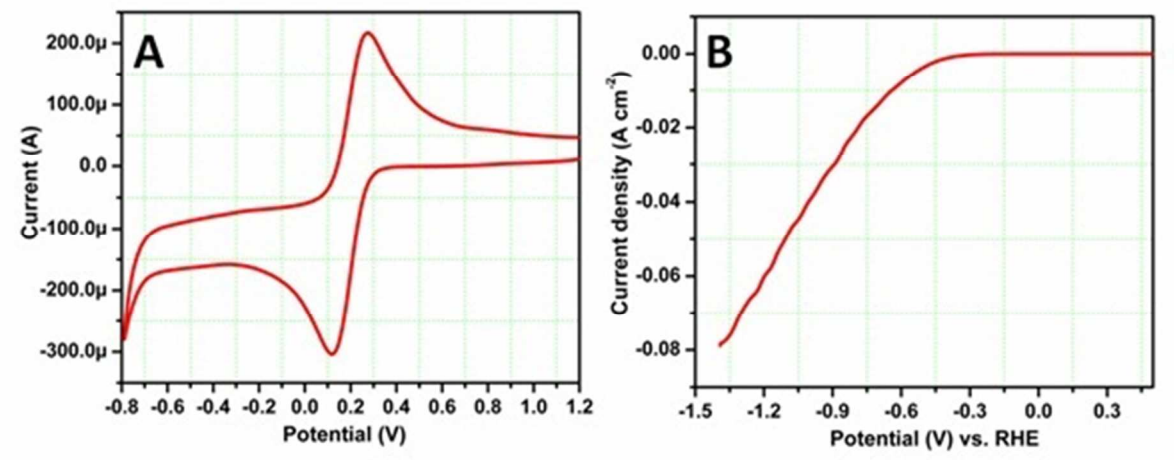

Figure S16: (A) CV runs for ferrocyanideand (B) LSV run towards HER, using $Er_2Si_2O_7$ modified PGE.

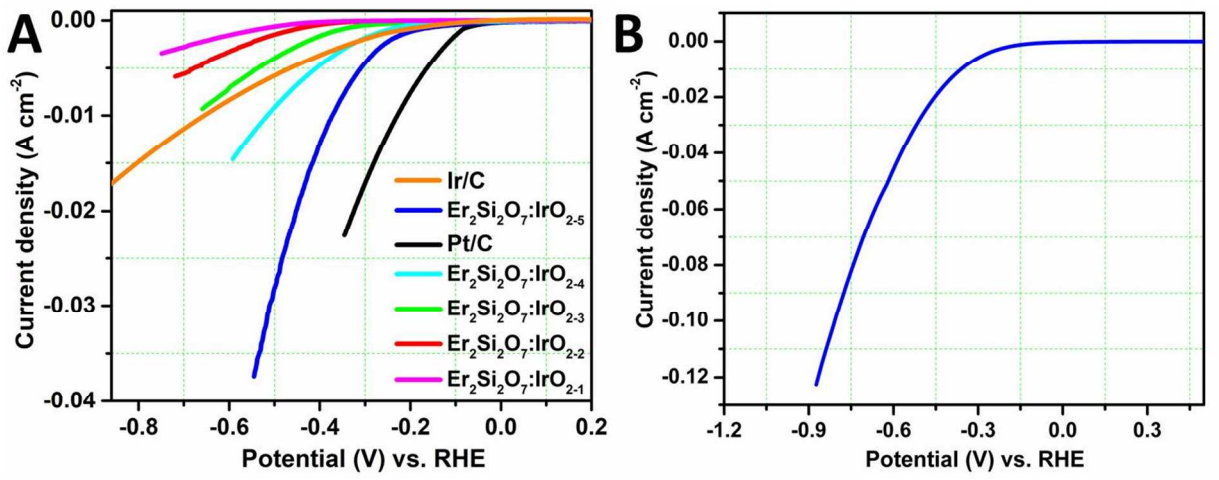

Figure S17:(A) HER performance of all catalyst normalized with respect to electrochemical surface area of IrO_2 modified PGE. (B) LSV run towards HER using IrO_2 modified PGE.